Published in final edited form as:

Neuropharmacology. 2020 May 15; 168: 107759. doi:10.1016/j.neuropharm.2019.107759.

Chronic intermittent ethanol exposure dysregulates a GABAergic microcircuit in the bed nucleus of the stria terminalis

Dipanwita Pati[a,#], **Catherine A. Marcinkiewicz**[a,#,1], **Jeffrey F. DiBerto**[b], **Elizabeth S. Cogan**[a], **Zoe A. McElligott**[a], **Thomas L. Kash**[a,b,*]

[a]Bowles Center for Alcohol Studies, University of North Carolina at Chapel Hill, Thurston Bowles Building 104 Manning Drive, Chapel Hill, NC, 27599, USA

[b]Department of Pharmacology, University of North Carolina School of Medicine, Chapel Hill, NC, 2751, USA

Abstract

Neuroadaptations in brain regions that regulate emotional and reward-seeking behaviors have been suggested to contribute to pathological behaviors associated with alcohol-use disorder. One such region is the bed nucleus of the stria terminalis (BNST), which has been linked to both alcohol consumption and alcohol withdrawal-induced anxiety and depression. Recently, we identified a GABAergic microcircuit in the BNST that regulates anxiety-like behavior. In the present study, we examined how chronic alcohol exposure alters this BNST GABAergic microcircuit in mice. We selectively targeted neurons expressing corticotropin releasing factor (CRF) using a CRF-reporter mouse line and combined retrograde labeling to identify BNST projections to the ventral tegmental area (VTA) and lateral hypothalamus (LH). Following 72 h of withdrawal from four weekly cycles of chronic intermittent ethanol (CIE) vapor exposure, the excitability of a sub-population of putative local CRF neurons that did not project to either VTA or LH ($CRF^{non\text{-}VTA/LH}$ neurons) was increased. Withdrawal from CIE also increased excitability of non-CRF BNST neurons that project to both LH and VTA ($BNST^{non\text{-}CRF\text{-}proj}$ neurons). Furthermore, both populations of neurons had a reduction in spontaneous EPSC amplitude while frequency was unaltered. Withdrawal from chronic alcohol was accompanied by a significant increase in spontaneous IPSC frequency selectively in the $BNST^{non\text{-}CRF\text{-}proj}$ neurons. Together, these data suggest that withdrawal from chronic ethanol dysregulates local CRF-GABAergic microcircuit to inhibit anxiolytic outputs of the BNST which may contribute to enhanced anxiety during alcohol withdrawal and drive alcohol-seeking behavior.

Keywords

Ethanol; BNST; VTA; LH; CRF; GABA

[*]**Corresponding author:** Thomas L. Kash, PhD, John R. Andrews Distinguished Professor, Bowles Center for Alcohol Studies, Department of Pharmacology, University of North Carolina School of Medicine, Chapel Hill, NC 27599, USA, tkash@email.unc.edu, Phone #: 919-966-7116.

[#]contributed equally to this work

[1]Present Address: Department of Pharmacology, Carver College of Medicine, University of Iowa College of Medicine, Iowa City, IA, 52242, USA

1. Introduction

A variety of factors contribute to the transition from controlled drinking to alcohol dependence, and a growing body of literature suggests that stress and anxiety play a critical role in this process (Koob, 2008; Sinha, 2008). Data from human studies indicate that stress can induce craving and relapse to substance abuse, and anxiety is a substantial risk factor for relapse in abstinent alcoholics (Breese et al, 2005; Fox et al, 2007; Hill et al, 2001; Sinha et al, 2008). In rodents, chronic ethanol exposure leads to increased anxiety-like behavior, as demonstrated by alterations in the novelty-induced suppression of feeding assay, the marble burying assay and the elevated plus maze assay (Jury et al, 2017; Pleil *et al*, 2015; Van Skike et al, 2015; for review, see, Kliethermes, 2005).

Converging evidence shows that the extended amygdala, particularly, the bed nucleus of the stria terminalis (BNST) plays a key role in anxiety-like behavior, stress-induced reinstatement of drug seeking, and negative affect related to dependence (Aston-Jones and Harris, 2004; Erb et al, 2001; for review, Lebow and Chen, 2016). The BNST comprises several sub-nuclei (Dong et al, 2001b, 2001a; Dong and Swanson, 2006a, 2006b) with the vast majority of neurons being GABAergic in phenotype (Sun and Cassell, 1993). The BNST sends both GABAergic and glutamatergic projections to areas known for reward-seeking and addiction, such as the ventral tegmental area (VTA) and the lateral hypothalamus (LH) (Dong and Swanson, 2006a, 2006b; Kudo et al, 2012; Jennings *et al*, 2013), and also has an extensive system of intrinsic, GABAergic interneurons (Sun and Cassell, 1993). Pharmacological manipulations within the BNST can alter ethanol drinking behaviors (Eiler II et al, 2003). Moreover, both acute and chronic ethanol exposure can induce persistent changes in the BNST circuit (Kash *et al*, 2008, 2009; Pleil et al, 2015a).

In addition to neurotransmitter releasing populations of neurons, BNST neurons can also co-express diverse neuropeptides that can robustly shape circuit function and behavior. One such peptide is corticotropin releasing factor (CRF), a 41-amino acid peptide that is co-expressed in GABAergic neurons within the BNST (Gray and Magnuson, 1992; Ju and Han, 1989). Within the BNST, CRF neurons are clustered in the dorsolateral and ventrolateral regions and dense CRF terminals are also expressed in the BNST, which may originate from either local BNST-CRF neurons or from BNST-projecting CRF neurons in the central amygdala (Cummings et al, 1983; Morin et al, 1999). Decades of research has implicated the role of the CRF system in alcohol addiction and stress- and anxiety-related behaviors (Heilig and Koob, 2007; Koob, 2008; Phillips et al, 2015). Central CRF signaling is recruited and altered in rodent models of alcohol dependence (Lowery-Gionta et al, 2012; Olive et al, 2002; Roberto et al, 2010; Silberman et al, 2013a). Previously, we have shown that inhibition of CRF neurons within the BNST, as well as BNST CRF neuron terminals in the VTA, suppresses binge alcohol drinking (Pleil et al, 2015c; Rinker et al, 2017).

Recently, we identified a BNST local GABAergic microcircuit that regulated anxiety-like behavior and fear learning via inhibition of BNST neurons that project to the VTA and LH (Marcinkiewcz et al, 2016). Using a combination of slice physiology and optogenetics, we found that a subpopulation of putative local CRF neurons that do not project to either the VTA or the LH (referred to as $CRF^{non\text{-}VTA/LH}$ neurons) inhibited BNST neurons that project

to the VTA and LH via GABA release. This inhibition resulted in increased anxiety-like behavior. While the importance of this BNST microcircuit in regulating anxiety-like behavior has been identified, it is not known how chronic alcohol exposure can alter the function of this microcircuit. Here we test the hypothesis that chronic ethanol exposure alters functional connectivity between $CRF^{non\text{-}VTA/LH}$ neurons and non-CRF BNST projections to the VTA and LH (referred to as $BNST^{non\text{-}CRF\text{-}proj}$ neurons), such that there is increased inhibition of BNST projections to the VTA and LH. To evaluate this, we used chronic intermittent ethanol (CIE) vapor exposure, a well-established rodent model of ethanol dependence and withdrawal (Becker and Lopez, 2004), and measured electrophysiological correlates of neuronal excitability and synaptic transmission in the BNST.

2. Materials and Methods

2.1. Mice

All experiments were performed on adult male mice (3-6 months) in accordance with the NIH guidelines for animal research and with the approval of the Institutional Animal Care and Use Committee at the University of North Carolina at Chapel Hill. Animals were group housed in a ventilated and temperature-controlled vivarium on a standard 12-hour cycle (lights on at 07:00) with *ad libitum* access to food and water. To visualize CRF-expressing neurons, Crf-ires-Cre mice (Krashes et al, 2014) were crossed with a Cre-inducible L10-GFP reporter line (Madisen et al, 2009) to produce CRF-L10A-GFP mice, referred to as CRF-reporters throughout the manuscript. CRF-reporters were bred in-house and mice were crossed for several generations to C57 mice before using.

2.2. Stereotaxic Surgery

All surgeries were done under aseptic conditions. Adult male mice were deeply anesthetized with 5% isoflurane (v/v) in oxygen and placed in a stereotactic frame (Kopf Instruments) while on a heated pad. To fluorescently label VTA- and LH-projecting BNST neurons, a retrograde tracer Choleratoxin B (CTB) 555 was microinjected bilaterally in the LH and the VTA using a 1 μl Neuros Hamilton syringe at a rate of 100 nl/min. CTB volume was 200 nl per target site. After infusion, the needle was left in place for 10 minutes to allow for diffusion of the CTB 555 before being slowly withdrawn. Injection coordinates (in mm, relative to bregma) used were: VTA (AP: −2.9, ML: ±0.3, DV: −4.6) and the LH (AP: −1.7, ML: ±0.9 to 1.10, DV: −5.00 to −5.2). Following surgery, all mice were returned to group housing and allowed to recover for at least two weeks before CIE exposure. Mice had *ad libitum* access to acetaminophen solution (0.4 mg/ml) two days before and seven days after surgery to minimize post-operative discomfort.

2.3. Chronic intermittent ethanol (CIE) exposure

Chronic ethanol exposure was achieved via vapor inhalation as previously described (Becker and Lopez, 2004; Jury et al, 2017). Briefly, two weeks post-surgery, mice were placed in vapor chambers and exposed to ethanol volatized by passing air through a vaporization stone submerged in ethanol (95%) and mixed with fresh air to deliver 19–22 mg ethanol/L of air at a rate of ~10 L/min. Mice in the ethanol group received i.p. injections of pyrazole (an alcohol dehydrogenase inhibitor) combined with 1.5 g/kg ethanol to induce intoxication and

stabilize blood ethanol concentrations prior to placement in the chambers. Air controls received only pyrazole and were placed in dedicated chambers (located adjacent to the ethanol chambers) in which air was exchanged at a rate of ~10 L/min.

Each cycle of CIE exposure lasted 16 h per day (in at 1700 h, out at 0900 h), followed by an 8 h withdrawal for four consecutive days of exposure (Monday-Friday) followed by a longer, 80 h, withdrawal (Friday-Monday). This was repeated for a total of four cycles.

2.4. Slice electrophysiology

For *ex vivo* slice physiology, mice were anesthetized with isoflurane, 72-hour post the last cycle of CIE and were rapidly decapitated. This time point was selected as we have previously observed behavioral changes at this time post CIE (Jury et al, 2017). 300 μm thick coronal sections through the BNST were prepared as previously described (Mazzone et al, 2016). Briefly, brains were quickly extracted, and slices were made using a Leica VT 1200s vibratome (Leica Biosystems, IL, USA) in ice-cold, oxygenated sucrose solution containing in mM: 194 sucrose, 20 NaCl, 4.4 KCl, 2 $CaCl_2$, 1 $MgCl_2$, 1.2 NaH_2PO_4, 10 glucose and 26 $NaHCO_3$ saturated with 95 % O_2/5 % CO_2. Slices were incubated for at least 30 minutes in normal artificial cerebral spinal fluid (ACSF) maintained at 32-35°C that contained in mM: 124 NaCl, 4.4 KCl, 1 NaH_2PO_4, 1.2 $MgSO_4$, 10 D-glucose, 2 $CaCl_2$, and 26 $NaHCO_3$, saturated with 95% O_2/5 % CO_2 before transferring to a submerged recording chamber (Warner Instruments, CT, USA) for experimental use. For whole-cell recordings, slices were continuously perfused at a rate of 1.5-2.0 ml/min with oxygenated ACSF maintained at 30±2°C.

Neurons were identified using infrared differential interference contrast on a Scientifica Slicescope II (East Sussex, UK). Fluorescent cells were visualized using a mercury arc lamp-based system combined with filters that allow for identification of GFP (470 nm), as well as red retrobeads (569 nm). Whole-cell patch clamp recordings were performed using micropipettes pulled from a borosilicate glass capillary tube using a Flaming/Brown electrode puller (Sutter P-97; Sutter Instruments, Novato, California). Electrode tip resistance was between 3 and 6 MΩ. All signals were acquired using an Axon Multiclamp 700B (Molecular Devices, Sunnyvale, CA). Data were sampled at 10 kHz, low-pass filtered at 3 kHz. Access resistance was continuously monitored and changes greater than 20% from the initial value were excluded from data analyses. Series resistance was uncompensated. 2-4 cells were recorded from each animal per set of experiments.

Excitability experiments were performed in current clamp mode using a potassium gluconate-based intracellular solution (in mM: 135 K-gluconate, 5 NaCl, 2 $MgCl_2$, 10 HEPES, 0.6 EGTA, 4 Na_2ATP, 0.4 Na_2GTP, pH 7.3, 285–292mOsm). Input resistance was measured immediately after breaking into the cell. Following stabilization, current was injected to hold cells at a common membrane potential of −70 mV to account for inter-cell variability. Changes in excitability were evaluated by measuring rheobase (minimum current required to elicit an action potential), action potential (AP) threshold and the number of action potentials fired at increasing 10 pA current steps (0 to 120 pA). Parameters related to AP shape, which included AP height, AP duration at half-maximal height (AP half-width),

time to fire an AP (AP latency), and afterhyperpolarization (AHP) amplitude were calculated from the first action potential fired during the V-I plot.

For assessment of spontaneous synaptic activity, two different intracellular solutions were used. Spontaneous excitatory postsynaptic currents (sEPSCs) were assessed in voltage clamp using a cesium gluconate-based internal (in mM: 135 Cs-gluconate, 5 NaCl, 10 HEPES, 0.6 EGTA, 4 ATP, 0.4 GTP, pH 7.2, 290–295 mOsm with 1mg/ml QX-314). Cells were voltage clamped at −80 mV in the presence of 25 μM picrotoxin (GABA-A receptor antagonist) to pharmacologically isolate EPSCs. Spontaneous inhibitory postsynaptic currents (sIPSCs) were pharmacologically isolated by adding kynurenic acid (3mM) to the ACSF to block AMPA and NMDA receptor-dependent postsynaptic currents. Cells were clamped at −70 mV and recorded using a potassium-chloride gluconate-based intracellular solution (in mM: 70 KCl, 65 K-gluconate, 5 NaCl, 10 HEPES, 0.5 EGTA, 4 ATP, 0.4 GTP, pH 7.2, 285–290mOsmol with 1mg/ml QX-314). For experiments that required minimal spontaneous synaptic activity in the slice, ACSF was supplemented with tetrodotoxin (TTX; 500 nM), to block voltage-gated sodium channels.

2.5. Drugs

All chemicals used for slice electrophysiology were obtained from either Tocris Bioscience (Minneapolis, USA) or Abcam (Cambridge, UK). CTB 555 was purchased from Invitrogen (Cat # C34776) and pyrazole from Sigma-Aldrich (St. Louis, MO, USA).

2.6. Data and statistical analysis

Differences in various electrophysiological measures were analyzed in Clampfit 10.6 or 10.7 (Molecular Devices, Sunnyvale, CA) and compared between the air and CIE-exposed groups. Frequency, amplitude, and kinetics of E/IPSCs were analyzed and visually confirmed using Clampfit 10.7. For comparisons between two groups, P-values were calculated using a standard unpaired t-test. If the condition of equal variances was not met, Welch's correction was used. Repeated measures ANOVAs (treatment X current injection) were used to assess between-group differences in the spike numbers fired across a range of current steps. All data are expressed as mean ± SEM. P-values ≤ 0.05 were considered significant. All statistical analysis was performed using GraphPad Prism v.8 (La Jolla, CA, USA).

3. Results

3.1. Withdrawal from CIE increases neuronal excitability of $CRF^{non\text{-}VTA/LH}$ neurons

The excitability of $CRF^{non\text{-}VTA/LH}$ neurons was assessed in CRF-reporter mice following 72h withdrawal from 4 cycles of CIE (Fig. 1A). $CRF^{non\text{-}VTA/LH}$ neurons were identified and differentiated from $BNST^{non\text{-}CRF\text{-}proj}$ neurons using a mercury arc lamp-based system. $CRF^{non\text{-}VTA/LH}$ neurons were defined as neurons that expressed GFP but not CTB 555. A total of six mice were used in each group to determine the excitability of $CRF^{non\text{-}VTA/LH}$ neurons following withdrawal from CIE. Fig 1C shows no change in resting membrane potential between air-exposed control mice (n=12 cells) and CIE-exposed mice (n=8 cells; [t(18)=0.6698, p=0.5115; unpaired t-test]). All measures of excitability were taken at −70

mV to normalize for inter-cell variability in RMP. The action potential threshold and the amount of current required to fire an action potential (rheobase) were assessed through a ramp protocol of 120 pA/1s. Withdrawal from CIE significantly reduced the rheobase when compared to air-exposed mice (Fig. 1B,D; n=13 cells in Air group; n=10 cells in CIE group; [t(15.65)=2.210, p=0.0424; unpaired t-test with Welch's correction) with no change in the action potential threshold (Fig. 1H; [t(21)= 1.247, p = 0.2260; unpaired t-test]). Next, we measured the number of action potentials fired across a range of current steps (0-120 pA for 250 ms, at an increment of 10 pA). We observed a significant interaction between the two groups as revealed by repeated measures two-way ANOVA (Fig. 1F-G; [F(12,252)=1.870, p=0.0385] for group x current interaction; [F(1,21)=3.062, p=0.0948] for main effect of group; [F(12,252)= 29.23, p<0.0001] for main effect of current). We also found that the average input resistance of $CRF^{non\text{-}VTA/LH}$ neurons obtained from CIE-exposed mice (n=10 cells) was higher when compared to air-exposed control mice (Fig.1E; n=13 cells; [t(21)= 2.438, p=0.0238; unpaired t-test]). The average capacitance did not differ between the two groups ([t(21)=0.3951, p=0.6968; unpaired t-test]). Also, there was a trend toward negative correlation between input resistance and rheobase in the CIE group (data not shown; r^2= 0.3383; p=0.0778). CIE did not alter action potential kinetics of $CRF^{non\text{-}VTA/LH}$ neurons. Specifically, CIE mice (n=10 cells) were similar to air mice (n=9 cells) with respect to AP latency (Fig. 1I; [t(17)=0.4339, p=0.6698; unpaired t-test]), peak AP amplitude (Fig. 1J; [t(17)=0.1742, p=0.8638; unpaired t-test]), AP half-width (Fig. 1J; [t(17)=0.1107, p=0.9131; unpaired t-test]) and fast AHP (Fig. 1K; n= 8 cells from Air group; n=9 cells from CIE group; [t(15)=0.8351, p=0.4168; unpaired t-test]). Together these results indicate that CIE results in increased excitability of a subpopulation of putatively local CRF expressing neurons in the BNST that do not project to LH and VTA.

3.2. Withdrawal from CIE increases neuronal excitability $BNST^{non\text{-}CRF\text{-}proj}$ neurons

We next asked whether CIE can modulate the excitability of $BNST^{non\text{-}CRF\text{-}proj}$ neurons. Four CRF-reporter mice per group were used for *ex-vivo* patch clamp recordings following CIE (Fig. 2A). $BNST^{non\text{-}CRF\text{-}proj}$ neurons were identified as neurons that expressed CTB 555 but not GFP. Mice that were exposed to air were similar to CIE-exposed mice with regard to RMP (Fig. 2C; n= 7 cells from Air controls; n=5 cells from CIE mice; [t(10)=1.022, p=0.3308; unpaired t-test]), input resistance (Fig. 2E; n= 7 cells from Air controls; n=6 cells from CIE mice; [t(11)=0.010, p=0.9917; unpaired t-test]), rheobase (Fig. 2B,D; [t(11)=0.4139, p=0.6869; unpaired t-test]) and action potential threshold (Fig. 2H; [t(11)=0.9363, p=0.3692; unpaired t-test]). Interestingly, we observed a significant interaction between the two groups and the number of action potentials fired across a range of current steps (Fig. 2F-G; [F(12, 132) = 2.412, p = 0.0074] for group x current interaction; [F(1,11) = 1.829, p=0.2034] for main effect of group; [F(12,132) = 72.17, p<0.0001] for main effect of current; RM measures two-way ANOVA). Similar to $CRF^{non\text{-}VTA/LH}$ neurons, there was no impact of CIE on action potential kinetics of $BNST^{non\text{-}CRF\text{-}proj}$ neurons as measured by AP latency (Fig. 2I; [t(11)=0.01708, p=0.9867; unpaired t-test]), AP height (Fig. 2J; [t(11)=1.368, p=0.1986; unpaired t-test]), AP half-width (Fig. 2J; [t(11)=1.499, p=0.1619; unpaired t-test]) and fast AHP (Fig. 2K; n= 6 cells per group; [t(10)=1.632, p=0.1338; unpaired t-test]). These data show increased excitability of non-CRF neurons in the BNST that project to LH and VTA in response to withdrawal from chronic ethanol.

3.3. Withdrawal from CIE reduces the amplitude of spontaneous, but not miniature, glutamatergic post-synaptic currents in both CRF$^{non\text{-}VTA/LH}$ and BNST$^{non\text{-}CRF\text{-}proj}$ neurons

Given that withdrawal from chronic ethanol could influence excitatory drive by altering glutamatergic signaling in the BNST, we evaluated the impact of CIE on excitatory synaptic transmission on both CRF$^{non\text{-}VTA/LH}$ and BNST$^{non\text{-}CRF\text{-}proj}$ neurons. CIE had no effect on sEPSC frequency onto CRF$^{non\text{-}VTA/LH}$ neurons (Fig. 3A-C; n=12 cells from 5 air-exposed mice and n=13 cells from 5 CIE-exposed mice; [t(23)=0.2927, p=0.7724; unpaired t-test]) but reduced the amplitude of sEPSC events ([t(16.60) =2.887, p=0.0104; unpaired t-test with Welch's correction]). Similarly, following CIE there was a significant reduction in sEPSC amplitude onto BNST$^{non\text{-}CRF\text{-}proj}$ neurons (Fig. 3F-H; n=12 cells from 5 air-exposed mice and n=11 cells from 6 CIE-exposed mice; [t(15.07)=3.725, p=0.0020; unpaired t-test with Welch's correction]) without altering the frequency ([t(21)=0.5680, p=0.5761; unpaired t-test]).

Surprisingly, this reduction in the amplitude of excitatory events in both population of neurons was not observed in action-potential independent miniature neurotransmission (in the presence of 500 nM tetrodotoxin). Specifically, no change in mEPSC frequency ([t(11.29)=0.9401, p=0.3669; unpaired t-test with Welch's correction]) and amplitude ([t(17)=0.5873, p=0.5647; unpaired t-test]) on CRF$^{non\text{-}VTA/LH}$ neurons (Fig. 3D-E; n=10 cells from 5 Air mice; n=9 cells from 4 CIE mice), neither any change in mEPSC frequency ([t(18)=0.017, p=0.9862; unpaired t-test]) and amplitude ([t(9.01)=0.1424, p=0.8899; unpaired t-test with Welch's correction]) on BNST$^{non\text{-}CRF\text{-}proj}$ neurons (Fig. 3I-J; n=9 cells in air group and n=11 cells in CIE group from 4 mice each). The average decay time (Air group: 3.439 ± 0.3415 ms; CIE group: 3.319 ± 0.3750 ms; [t(17)=0.2356, p=0.8166; unpaired t-test]) and rise time (Air group: 1.275 ±0.07970 ms; CIE group: 1.152 ± 0.08545 ms; [t(17) =1.051, p=0.3080; unpaired t-test]) of mEPSC on CRF$^{non\text{-}VTA/LH}$ neurons did not vary between the two groups. Similarly, the average decay time (Air group: 3.183 ± 0.3933 ms; CIE group: 3.574 ± 0.3478 ms; [t(18)=0.7455, p=0.4656; unpaired t-test]) and rise time (Air group: 1.304 ± 0.1034 ms; CIE group: 1.116 ± 0.066 ms; [t(18)=1.589, p=0.1294; unpaired t-test]) of mEPSC on BNST$^{non\text{-}CRF\text{-}proj}$ neurons were not altered by exposure to chronic ethanol. Thus, withdrawal from CIE modulated action potential-dependent glutamatergic transmission on both CRF$^{non\text{-}VTA/LH}$ and BNST$^{non\text{-}CRF\text{-}proj}$ neurons.

3.4 Withdrawal from CIE selectively increases GABAergic transmission on BNST$^{non\text{-}CRF\text{-}proj}$ neurons, but not on CRF$^{non\text{-}VTA/LH}$ neurons

Based on previous work from our lab suggesting that CRF neurons form local inhibitory circuits within the BNST, we next measured GABAergic signaling in both CRF$^{non\text{-}VTA/LH}$ and BNST$^{non\text{-}CRF\text{-}proj}$ neurons after CIE. Withdrawal from CIE did not alter sIPSCs in CRF$^{non\text{-}VTA/LH}$ neurons, with no change in either frequency (Fig. 4A-B; n=10-11 cells from 5 mice in each group; [t(19)=0.4209, p=0.6785; unpaired t-test]) or amplitude (Fig. 4C; [t(19)=0.8925, p=0.3833; unpaired t-test]). Also, no change was observed in either action-potential independent (miniature) IPSC (mIPSC) frequency onto CRF$^{non\text{-}VTA/LH}$ neurons (Fig. 4D-E; n= 9 cells each from 4 air-exposed mice and 5 CIE-exposed mice, respectively; [t(16)=0.4685, p=0.6458; unpaired t-test]) or mIPSC amplitude ([t(16)=1.342, p=0.1982; unpaired t-test]). Additionally, we did not observe any change in mIPSC kinetics such as,

average decay time (Air group: 23.59 ± 1.969 ms; CIE group: 22.73 ± 2.270 ms; [t(16)=0.2853, p=0.7791; unpaired t-test]) and rise time (Air group: 2.573 ± 0.1986 ms; CIE group: 2.829 ± 0.1792 ms; [t(16)=0.9553, p=0.3536; unpaired t-test]).

In contrast, $BNST^{non\text{-}CRF\text{-}proj}$ neurons had a significant upregulation in GABAergic signaling as indicated by an increase in sIPSC frequency (Fig. 4F-G; n=11 cells from 3 air mice and n=19 cells from 4 CIE mice; [t(23.22)=3.929, p=0.0007; unpaired t-test with Welch's correction]) but not amplitude (Fig. 4H; [t(28)=0.3091, p=0.7595; unpaired t-test]). This change was dependent on the action-potential mediated release of GABA since the effect was blocked in the presence of TTX (Fig. 4I-J; n= 12 cells from 6 Air mice and n= 7 cells from 3 CIE mice; [t(6.963)=0.6961, p=0.5089; unpaired t-test with Welch's correction]). No change was observed in mIPSC amplitude on $BNST^{non\text{-}CRF\text{-}proj}$ neurons ([t(17)=1.023, p=0.3209; unpaired t-test]). Further, we did not find any change in either decay time (Air group: 21.37 ± 1.068 ms; CIE group: 19.87 ± 1.477 ms; [t(17)=0.8352, p=0.4152; unpaired t-test]) or rise time (Air group: 2.044 ± 0.1236 ms; CIE group: 2.264 ± 0.2588 ms; [t(17)=0.8686, p=0.3971; unpaired t-test]) of mIPSCs. Collectively, these data reveal a selective increase in an inhibitory drive on $BNST^{non\text{-}CRF\text{-}proj}$ neurons in mice undergoing withdrawal from CIE mice that is network activity-dependent.

4. Discussion

The BNST is a key integrator of diverse motivational states (Lebow and Chen, 2016) and plays a critical role in addiction-related behavior (Carboni et al, 2000; Koob and Le Moal, 2008). Here we show that chronic exposure to ethanol followed by 72h withdrawal leads to robust changes in neuronal function consistent with engagement of a local GABAergic microcircuit in the BNST, supporting a role for this circuit in the pathophysiology of alcohol abuse. We used the CIE model (Becker and Lopez, 2004) as CIE has been shown to elicit robust alterations in the physiology of the BNST (Kash et al, 2009; Wills et al, 2012; Marcinkiewcz et al, 2015; Pleil et al, 2015b) and anxiety-like behavior. We focused on two distinct populations of neurons within the BNST characterized by their neuropeptide expression and outputs. $CRF^{non\text{-}VTA/LH}$ neurons were defined as BNST neurons that expressed the neuropeptide, CRF, and did not project to either the VTA or the LH. $BNST^{non\text{-}CRF\text{-}proj}$ neurons were identified as BNST neurons that send projections to the VTA or the LH and do not express CRF. Withdrawal from chronic ethanol exposure increased the excitability of both $CRF^{non\text{-}VTA/LH}$ and $BNST^{non\text{-}CRF\text{-}proj}$ neurons. Additionally, both $CRF^{non\text{-}VTA/LH}$ and $BNST^{non\text{-}CRF\text{-}proj}$ neurons had a reduction in the amplitude of excitatory transmission following withdrawal. Interestingly, this effect was activity-dependent and did not alter action-potential independent transmission. Furthermore, we show that ethanol withdrawal significantly increased inhibitory transmission specifically in $BNST^{non\text{-}CRF\text{-}proj}$ neurons that depended on within slice network dynamics. Taken together, these results demonstrate that withdrawal from chronic ethanol exposure dysregulates local CRF-GABAergic microcircuit which may contribute to the alcohol-induced negative affect and drive craving and alcohol-seeking behavior.

4.1 Chronic ethanol effects on CRF$^{non\text{-}VTA/LH}$ neurons in the BNST

CRF, a stress peptide plays an integral role in modulating alcohol addiction and stress- and anxiety-related behaviors (Heilig and Koob, 2007; Koob, 2008; Phillips et al, 2015). CRF signaling through G-protein coupled receptors CRFR1 and CRFR2 is engaged in rodent models of alcohol dependence (Lowery-Gionta et al, 2012; Olive et al, 2002; Roberto et al, 2010). Within the BNST, CRF neurons are clustered in the dorsolateral and ventrolateral regions (Silberman et al, 2013b) with dense CRF terminals originating from either local CRF neurons or from BNST-projecting CRF neurons in the central amygdala (Cummings et al, 1983; Morin et al, 1999). CRF levels in the BNST are elevated during withdrawal from alcohol (Olive et al, 2002). Inhibition of CRF neurons within the BNST has been shown to suppress binge alcohol drinking (Pleil et al, 2015c; Rinker et al, 2017). Recently, we identified a subset of CRF-expressing BNST neurons that do not project to either the VTA or the LH (CRF$^{non\text{-}VTA/LH}$ neurons) were directly depolarized by serotonin and increased anxiety-like behavior (Marcinkiewcz et al, 2016).

In the present study we hypothesized that withdrawal from chronic ethanol results in hyperexcitability of CRF$^{non\text{-}VTA/LH}$ neurons that may contribute to withdrawal-induced anxiety. We found an increase in neuronal excitability of CRF$^{non\text{-}VTA/LH}$ neurons that was associated with lowering of the threshold for action potential initiation and greater spike frequency in response to current injection. Furthermore, we observed an increase in input resistance in CRF$^{non\text{-}VTA/LH}$ neurons from the CIE-exposed animals. Similar changes in intrinsic excitability following CIE have been observed in the BNST (Marcinkiewcz et al, 2015; Pleil *et al*, 2015). Marcinkiewcz et al, 2015, found an increase in excitability of ventral BNST neurons which was dependent on activation of 5HT2C receptors. Also, neuromodulators such as dopamine and noradrenaline have been shown to directly depolarize CRF neurons (Silberman et al, 2013b). Thus, future work should look at whether different neuromodulators are involved in the increased excitability of CRF$^{non\text{-}VTA/LH}$ neurons and whether the increased excitability observed in CRF$^{non\text{-}VTA/LH}$ neurons could promote anxiety-like behavior during ethanol withdrawal.

Following 72 h withdrawal from chronic ethanol exposure, we did not observe any changes in either frequency or amplitude of inhibitory synaptic transmission in CRF$^{non\text{-}VTA/LH}$ neurons. Interestingly, we found a reduction in the amplitude of spontaneous glutamatergic transmission without any alterations in frequency. This effect was dependent on action-potential mediated glutamate release since the increase in amplitude was occluded in the presence of tetrodotoxin. This suggests ethanol-induced reduction in glutamatergic amplitude involves unknown factors that are dependent on within-slice network dynamics. One intriguing possibility is that in alcohol exposed mice there is release of a neuromodulatory factor such as a neuropeptide that alters glutamatergic transmission. This is noteworthy as studies from the Winder lab have found that alcohol exposure can lead to engagement of CRF signaling in the BNST (Silberman et al, 2013b), it may be that CRF plays a role in this process, which could be explored with either genetics or pharmacology. Further, previous work from McElligott et al, 2010 showed an impairment of α1-adrenergic receptor-dependent long-term depression of glutamate signaling in the BNST in mice chronically exposed to ethanol. Additionally, this α1 receptor-mediated plasticity was

associated with a decrease in amplitude of events with spontaneous glutamatergic transmission but not with miniature transmission.

4.2 Modulation of the BNST$^{non\text{-}CRF}$ neurons that project to the VTA or the LH

The BNST sends predominantly GABAergic but also sparse glutamatergic projections to the VTA (Georges and Aston-Jones, 2002; Jalabert et al, 2009). Activation of BNST GABAergic terminals in the VTA is anxiolytic and rewarding, while activation of glutamatergic terminals in the VTA is aversive (Jennings et al, 2013b). Also, work from our lab demonstrated serotonin-mediated inhibition of VTA projecting BNST neurons result in increased anxiety and fear learning (Marcinkiewcz et al, 2016). In addition, there is also a BNST-CRFergic projection to VTA (Rodaros et al, 2007) which can regulate binge-like drinking (Rinker et al, 2017) and anxiety-like behavior (Marcinkiewcz et al, 2016). Additionally, BNST sends robust projections to the LH (Dong and Swanson, 2004). While activation of BNST-GABAergic terminals in the LH produced robust feeding behavior (Jennings et al, 2013a), stimulation of anterodorsal BNST inputs to the LH resulted in anxiolysis without affecting reward-related behaviors (Kim et al, 2013). Recently, Giardino et al, 2018 characterized two non-overlapping GABAergic pathways from BNST to LH that promote divergent emotional states. A limitation of our study is that we specifically did not record from BNST CRF neurons that project to the VTA and LH. Notably, we also did not determine the neurochemical phenotype of the non-CRF neurons that project to the VTA or the LH. Our rationale was that the GABAergic output is the predominant output. However, it is possible that in our recordings we recorded from glutamatergic neurons that project to the VTA. If this were the case, the increase in excitability of glutamate output neurons to the VTA would serve to promote aversion (Jennings et al, 2013b). Future work could pair a mouse that expresses flp in CRF neurons with vGAT-cre and vGlut-cre mouse lines to more rigorously explore the connectivity between CRF and these distinct VTA outputs, and the impact of alcohol on these populations.

Several studies have implicated BNST projections to the VTA and the LH in addiction-like behavior (Aston-Jones and Harris, 2004; Mahler and Aston-Jones, 2012; Sartor and Aston-Jones, 2012). Here, we hypothesized that withdrawal from chronic ethanol results in increased inhibition of BNST$^{non\text{-}CRF\text{-}proj}$ neurons to induce an aversive state that may contribute to negative affect-driven alcohol-seeking behavior. First, we observed a leftward shift in the spike frequency in response to current injection in CIE-exposed mice. This shift was not associated with alterations in any other parameters of intrinsic excitability. We also observed a reduction in the amplitude of spontaneous glutamatergic transmission. Similar to CRF$^{non\text{-}VTA/LH}$ neurons, this effect was dependent on network activity. Prior work from Silberman et al, 2013a reported an increase in the frequency of spontaneous excitatory currents on VTA-projecting BNST neurons following CIE. We did not observe any change in the frequency of either spontaneous or miniature excitatory events. A possible explanation for the lack of increase in glutamatergic signaling in the BNST$^{non\text{-}CRF\text{-}proj}$ neurons is the duration of withdrawal prior to slice physiology. While Silberman et al, 2013a looked at changes following acute withdrawal (4 h after last CIE session) our experiments were conducted 72 h post CIE. Acute withdawal is associated with a hyperglutamatergic state and

thus could explain the increased glutamate signaling on VTA-projecting BNST neurons in contrast to no change as observed post 72 h withdrawal.

Adaptations in the GABAergic signaling have been suggested to regulate various aspects of acute and protracted withdrawal (Davies, 2003). Chronic ethanol has been shown to significantly alter GABAergic signaling in various brain regions, including the extended amygdala (Herman et al, 2016; Roberto et al, 2003, 2010; Pleil et al, 2015c). In the central amygdala, chronic ethanol administration enhances basal GABAergic transmission and GABA release as measured by microdialysis and electrophysiology techniques (Roberto et al, 2004). Here we report an increase in basal GABAergic transmission on $BNST^{non\text{-}CRF\text{-}proj}$ neurons following withdrawal from CIE. We observed an increase in the frequency of spontaneous inhibitory events without changes in the amplitude of events suggesting a putative presynaptic increase in GABA release. Interestingly, this effect was abolished in the absence of action-potential dependent neurotransmission. Taken together with the changes in the excitability of putative local $BNST^{CRF}$ neurons, this suggests that withdrawal from CIE leads to engagement of this microcircuit. Curiously, despite an increase in GABAergic transmission in $BNST^{non\text{-}CRF\text{-}Proj}$, we did not observe any reduction in excitability, as may be expected. One potentially interesting possibility is that a long-term change in GABAergic transmission in these neurons induces a homeostatic shift in excitability, as has been identified in cell culture experiments (Joseph and Turrigiano, 2017).

4.3 Functional implications

Previously, we identified a subset of CRF neurons that do not project to either the VTA or the LH and can inhibit VTA- and LH-projecting BNST neurons to enhance anxiety-like behavior (Marcinkiewcz et al, 2016). In the present study, the two most important findings are 1) increased excitability of $CRF^{non\text{-}VTA/LH}$ neurons, 2) increased activity-dependent GABAergic inhibition of $BNST^{non\text{-}CRF\text{-}proj}$ neurons following withdrawal from CIE. Thus, a plausible mechanism is withdrawal-induced excitation of $CRF^{non\text{-}VTA/LH}$ neurons which results in increased GABA release onto $BNST^{non\text{-}CRF\text{-}proj}$ neurons. The net effect of ethanol-induced dysregulation of this microcircuit is inhibition of BNST-projections to the VTA and the LH which could drive negative behavioral states, leading potentially to increased anxiety and dysphoria. While this is the most parsimonious explanation of our data, there are some caveats to the present study. The two non-overlapping subpopulations of neurons were identified using a combination of genetic and retrograde labeling techniques. Retrograde based labeling can vary between animals and there is a possibility that putative ‘non-projecting’ neurons actually do project to the VTA but do not have sufficient uptake of retrobeads for detection in our experimental setup. In the future, genetic tools like INTRSECT (Intronic Recombinase Sites Enabling Combinatorial Targeting) could be used to isolate specific populations with higher accuracy (Marcinkiewcz et al, 2016). Another important factor is the anatomical location of the recorded neurons. Our dataset is a combination of neurons from the dorsal and the ventral nuclei of BNST. Given the heterogeneity of modulatory inputs into different sub nuclei of BNST (McElligott and Winder, 2009), this could impact the interpretation of the data. For example, while the dorsal BNST receives a robust dopamine input (Freedman and Cassell, 1994), the ventral BNST

receives a larger noradrenergic input (Forray and Gysling, 2004). It is plausible that because of this, recordings in these different regions are reflective of different plasticity processes.

Prior work from our group (Jury et al, 2017) has shown sex-specific differences in ethanol-related behaviors using CIE as a model of dependence. Since, all our experiments were conducted in male mice, future work should examine the neural consequences of withdrawal from CIE in female mice. Altogether, our data provide electrophysiological correlates of ethanol withdrawal-induced modulation of this local GABAergic microcircuit and shed additional insight to neural mechanisms underlying the pathophysiology of alcoholism. The behavioral impact of this alcohol-induced dysregulation of the BNST CRF-GABAergic microcircuit is a potentially interesting future direction.

5. Conclusions

Withdrawal from repeated cycles of intermittent ethanol exposure results in the hyperexcitability of a sub-population of CRF neurons while increasing inhibitory drive on non-CRF BNST neurons that project to both the LH and the VTA. Chronic alcohol mediated dysregulation of this microcircuit can likely alter the activity of VTA- and LH-projecting outputs of the BNST contributing to increased anxiety-like behavior and alcohol consumption. Collectively, these results enhance our understanding of the role of neuropeptide- and projection-specific plasticity in the BNST that can drive relapse and alcohol seeking.

Acknowledgments

Funding and Disclosure: This work was funded by NIAAA grants R01 AA019454 (TLK), U01 AA020911 (TLK), P60 AA011605 (TLK), U24 AA025475 and K99A024215 (CAM). The authors declare no conflicts of interest.

6. References

Aston-Jones G, Harris GC (2004). Brain substrates for increased drug seeking during protracted withdrawal. Neuropharmacology 47: 167–179. [PubMed: 15464135]

Becker HC, Lopez MF (2004). Increased Ethanol Drinking After Repeated Chronic Ethanol Exposure and Withdrawal Experience in C57BL/6 Mice. Alcohol Clin Exp Res 28: 1829–1838. [PubMed: 15608599]

Breese GR, Chu K, Dayas CV, Funk D, Knapp DJ, Koob GF, et al. (2005). Stress Enhancement of Craving During Sobriety: A Risk for Relapse. Alcohol Clin Exp Res 29: 185–195. [PubMed: 15714042]

Carboni E, Silvagni A, Rolando MTP, Di Chiara G (2000). Stimulation of In Vivo Dopamine Transmission in the Bed Nucleus of Stria Terminalis by Reinforcing Drugs. J Neurosci 20: RC102 LP – RC102. [PubMed: 11027253]

Cummings S, Elde R, Ells J, Lindall A (1983). Corticotropin-releasing factor immunoreactivity is widely distributed within the central nervous system of the rat: an immunohistochemical study. J Neurosci 3: 1355 LP – 1368. [PubMed: 6345725]

Davies M (2003). The role of GABAA receptors in mediating the effects of alcohol in the central nervous system. J Psychiatry Neurosci 28: 263–274. [PubMed: 12921221]

Dong H-W, Petrovich GD, Watts AG, Swanson LW (2001a). Basic organization of projections from the oval and fusiform nuclei of the bed nuclei of the stria terminalis in adult rat brain. J Comp Neurol 436: 430–455. [PubMed: 11447588]

Dong H-W, Swanson LW (2004). Organization of axonal projections from the anterolateral area of the bed nuclei of the stria terminalis. J Comp Neurol 468: 277–298. [PubMed: 14648685]

Dong H-W, Swanson LW (2006a). Projections from bed nuclei of the stria terminalis, dorsomedial nucleus: Implications for cerebral hemisphere integration of neuroendocrine, autonomic, and drinking responses. J Comp Neurol 494: 75–107. [PubMed: 16304681]

Dong H-W, Swanson LW (2006b). Projections from bed nuclei of the stria terminalis, anteromedial area: Cerebral hemisphere integration of neuroendocrine, autonomic, and behavioral aspects of energy balance. J Comp Neurol 494: 142–178. [PubMed: 16304685]

Dong HW, Petrovich GD, Swanson LW (2001b). Topography of projections from amygdala to bed nuclei of the stria terminalis. Brain Res Rev 38: 192–246. [PubMed: 11750933]

Eiler WJA II, Seyoum R, Foster KL, Mailey C, June HL (2003). D1 dopamine receptor regulates alcohol-motivated behaviors in the bed nucleus of the stria terminalis in alcohol-preferring (P) rats. Synapse 48: 45–56. [PubMed: 12557272]

Erb S, Shaham Y, Stewart J (2001). Stress-induced Relapse to Drug Seeking in the Rat; Role of the Bed Nucleus of the Stria Terminalis and Amygdala. Stress 4: 289–303. [PubMed: 22432148]

Forray MI, Gysling K (2004). Role of noradrenergic projections to the bed nucleus of the stria terminalis in the regulation of the hypothalamic–pituitary–adrenal axis. Brain Res Rev 47: 145–160. [PubMed: 15572169]

Fox HC, Bergquist KL, Hong K-I, Sinha R (2007). Stress-Induced and Alcohol Cue-Induced Craving in Recently Abstinent Alcohol-Dependent Individuals. Alcohol Clin Exp Res 31: 395–403. [PubMed: 17295723]

Freedman LJ, Cassell MD (1994). Distribution of dopaminergic fibers in the central division of the extended amygdala of the rat. Brain Res 633: 243–252. [PubMed: 7511034]

Georges F, Aston-Jones G (2002). Activation of ventral tegmental area cells by the bed nucleus of the stria terminalis: a novel excitatory amino acid input to midbrain dopamine neurons. J Neurosci 22: 5173–87. [PubMed: 12077212]

Giardino WJ, Eban-Rothschild A, Christoffel DJ, Li S-B, Malenka RC, de Lecea L (2018). Parallel circuits from the bed nuclei of stria terminalis to the lateral hypothalamus drive opposing emotional states. Nat Neurosci 21: 1084–1095. [PubMed: 30038273]

Gray TS, Magnuson DJ (1992). Peptide immunoreactive neurons in the amygdala and the bed nucleus of the stria terminalis project to the midbrain central gray in the rat. Peptides 13: 451–460. [PubMed: 1381826]

Heilig M, Koob GF (2007). A key role for corticotropin-releasing factor in alcohol dependence. Trends Neurosci 30: 399–406. [PubMed: 17629579]

Herman MA, Contet C, Roberto M (2016). A Functional Switch in Tonic GABA Currents Alters the Output of Central Amygdala Corticotropin Releasing Factor Receptor-1 Neurons Following Chronic Ethanol Exposure. J Neurosci 36: 10729 LP – 10741. [PubMed: 27798128]

Hill A, Junghanns K, Driessen M, Meier S, Wetterling T, Lange W (2001). The course of anxiety, depression and drinking behaviours after completed detoxification in alcoholics with and without comorbid anxiety and depressive disorders. Alcohol Alcohol 36: 249–255. [PubMed: 11373263]

Jalabert M, Aston-Jones G, Herzog E, Manzoni O, Georges F (2009). Role of the bed nucleus of the stria terminalis in the control of ventral tegmental area dopamine neurons. Prog Neuro-Psychopharmacology Biol Psychiatry 33: 1336–1346.

Jennings JH, Rizzi G, Stamatakis AM, Ung RL, Stuber GD (2013a). The inhibitory circuit architecture of the lateral hypothalamus orchestrates feeding. Science (80-) 341: 1517–1521.

Jennings JH, Sparta DR, Stamatakis AM, Ung RL, Pleil KE, Kash TL, et al. (2013b). Distinct extended amygdala circuits for divergent motivational states. Nature 496: 224. [PubMed: 23515155]

Joseph A, Turrigiano GG (2017). All for One But Not One for All: Excitatory Synaptic Scaling and Intrinsic Excitability Are Coregulated by CaMKIV, Whereas Inhibitory Synaptic Scaling Is Under Independent Control. J Neurosci 37: 6778 LP – 6785. [PubMed: 28592691]

Ju G, Han Z (1989). Coexistence of corticotropin releasing factor and neurotensin within oval nucleus neurons in the bed nuclei of the stria terminalis in the rat. Neurosci Lett 99: 246–250. [PubMed: 2657507]

Jury NJ, DiBerto JF, Kash TL, Holmes A (2017). Sex differences in the behavioral sequelae of chronic ethanol exposure. Alcohol 58: 53–60. [PubMed: 27624846]

Kash TL, Baucum AJ II, Conrad KL, Colbran RJ, Winder DG (2009). Alcohol Exposure Alters NMDAR Function in the Bed Nucleus of the Stria Terminalis. Neuropsychopharmacology 34: 2420. [PubMed: 19553918]

Kash TL, Matthews RT, Winder DG (2007). Alcohol Inhibits NR2B-Containing NMDA Receptors in the Ventral Bed Nucleus of the Stria Terminalis. Neuropsychopharmacology 33: 1379. [PubMed: 17625498]

Kim S-Y, Adhikari A, Lee SY, Marshel JH, Kim CK, Mallory CS, et al. (2013). Diverging neural pathways assemble a behavioural state from separable features in anxiety. Nature 496: 219. [PubMed: 23515158]

Kliethermes CL (2005). Anxiety-like behaviors following chronic ethanol exposure. Neurosci Biobehav Rev 28: 837–850. [PubMed: 15642625]

Koob GF (2008). A Role for Brain Stress Systems in Addiction. Neuron 59: 11–34. [PubMed: 18614026]

Koob GF, Le Moal M (2008). Review. Neurobiological mechanisms for opponent motivational processes in addiction. Philos Trans R Soc Lond B Biol Sci 363: 3113–3123. [PubMed: 18653439]

Krashes MJ, Shah BP, Madara JC, Olson DP, Strochlic DE, Garfield AS, et al. (2014). An excitatory paraventricular nucleus to AgRP neuron circuit that drives hunger. Nature 507: 238. [PubMed: 24487620]

Kudo T, Uchigashima M, Miyazaki T, Konno K, Yamasaki M, Yanagawa Y, et al. (2012). Three Types of Neurochemical Projection from the Bed Nucleus of the Stria Terminalis to the Ventral Tegmental Area in Adult Mice. J Neurosci 32: 18035 LP – 18046. [PubMed: 23238719]

Lebow MA, Chen A (2016). Overshadowed by the amygdala: The bed nucleus of the stria terminalis emerges as key to psychiatric disorders. Mol Psychiatry 21: 450–463. [PubMed: 26878891]

Lowery-Gionta EG, Navarro M, Li C, Pleil KE, Rinker JA, Cox BR, et al. (2012). Corticotropin Releasing Factor Signaling in the Central Amygdala is Recruited during Binge-Like Ethanol Consumption in C57BL/6J Mice. J Neurosci 32: 3405 LP – 3413. [PubMed: 22399763]

Madisen L, Zwingman TA, Sunkin SM, Oh SW, Zariwala HA, Gu H, et al. (2009). A robust and high-throughput Cre reporting and characterization system for the whole mouse brain. Nat Neurosci 13: 133. [PubMed: 20023653]

Mahler SV, Aston-Jones GS (2012). Fos activation of selective afferents to ventral tegmental area during cue-induced reinstatement of cocaine seeking in rats. J Neurosci 32: 13309–13325. [PubMed: 22993446]

Marcinkiewcz CA, Dorrier CE, Lopez AJ, Kash TL (2015). Ethanol induced adaptations in 5-HT2c receptor signaling in the bed nucleus of the stria terminalis: Implications for anxiety during ethanol withdrawal. Neuropharmacology 89: 157–167. [PubMed: 25229718]

Marcinkiewcz CA, Mazzone CM, D'Agostino G, Halladay LR, Hardaway JA, DiBerto JF, et al. (2016). Serotonin engages an anxiety and fear-promoting circuit in the extended amygdala. Nature 537: 97. [PubMed: 27556938]

Mazzone CM, Pati D, Michaelides M, DiBerto J, Fox JH, Tipton G, et al. (2016). Acute engagement of Gq-mediated signaling in the bed nucleus of the stria terminalis induces anxiety-like behavior. Mol Psychiatry 23: 143. [PubMed: 27956747]

McElligott ZA, Klug JR, Nobis WP, Patel S, Grueter BA, Kash TL, et al. (2010). Distinct forms of G_q-receptor-dependent plasticity of excitatory transmission in the BNST are differentially affected by stress. Proc Natl Acad Sci 107: 2271 LP – 2276. [PubMed: 20133871]

McElligott ZA, Winder DG (2009). Modulation of glutamatergic synaptic transmission in the bed nucleus of the stria terminalis. Prog Neuro-Psychopharmacology Biol Psychiatry 33: 1329–1335.

Morin SM, Ling N, Liu X-J, Kahl SD, Gehlert DR (1999). Differential distribution of urocortin- and corticotropin-releasing factor-like immunoreactivities in the rat brain. Neuroscience 92: 281–291. [PubMed: 10392850]

Olive MF, Koenig HN, Nannini MA, Hodge CW (2002). Elevated extracellular CRF levels in the bed nucleus of the stria terminalis during ethanol withdrawal and reduction by subsequent ethanol intake. Pharmacol Biochem Behav 72: 213–220. [PubMed: 11900791]

Phillips TJ, Reed C, Pastor R (2015). Preclinical evidence implicating corticotropin-releasing factor signaling in ethanol consumption and neuroadaptation. Genes, Brain Behav 14: 98–135. [PubMed: 25565358]

Pleil KE, Lowery-Gionta EG, Crowley NA, Li C, Marcinkiewcz CA, Rose JH, et al. (2015a). Effects of chronic ethanol exposure on neuronal function in the prefrontal cortex and extended amygdala. Neuropharmacology 99: 735–749. [PubMed: 26188147]

Pleil KE, Lowery-Gionta EG, Crowley NA, Li C, Marcinkiewcz CA, Rose JH, et al. (2015b). Effects of chronic ethanol exposure on neuronal function in the prefrontal cortex and extended amygdala. Neuropharmacology 99: 735–749. [PubMed: 26188147]

Pleil KE, Rinker JA, Lowery-Gionta EG, Mazzone CM, McCall NM, Kendra AM, et al. (2015c). NPY signaling inhibits extended amygdala CRF neurons to suppress binge alcohol drinking. Nat Neurosci 18: 545. [PubMed: 25751534]

Rinker JA, Marshall SA, Mazzone CM, Lowery-Gionta EG, Gulati V, Pleil KE, et al. (2017). Extended Amygdala to Ventral Tegmental Area Corticotropin-Releasing Factor Circuit Controls Binge Ethanol Intake. Biol Psychiatry 81: 930–940. [PubMed: 27113502]

Roberto M, Cruz MT, Gilpin NW, Sabino V, Schweitzer P, Bajo M, et al. (2010). Corticotropin Releasing Factor–Induced Amygdala Gamma-Aminobutyric Acid Release Plays a Key Role in Alcohol Dependence. Biol Psychiatry 67: 831–839. [PubMed: 20060104]

Roberto M, Madamba SG, Moore SD, Tallent MK, Siggins GR (2003). Ethanol increases GABAergic transmission at both pre- and postsynaptic sites in rat central amygdala neurons. Proc Natl Acad Sci 100: 2053 LP – 2058. [PubMed: 12566570]

Roberto M, Madamba SG, Stouffer DG, Parsons LH, Siggins GR (2004). Increased GABA Release in the Central Amygdala of Ethanol-Dependent Rats. J Neurosci 24: 10159 LP – 10166. [PubMed: 15537886]

Rodaros D, Caruana DA, Amir S, Stewart J (2007). Corticotropin-releasing factor projections from limbic forebrain and paraventricular nucleus of the hypothalamus to the region of the ventral tegmental area. Neuroscience 150: 8–13. [PubMed: 17961928]

Sartor GC, Aston-Jones G (2012). Regulation of the ventral tegmental area by the bed nucleus of the stria terminalis is required for expression of cocaine preference. Eur J Neurosci 36: 3549–3558. [PubMed: 23039920]

Silberman Y, Matthews RT, Winder DG (2013a). A Corticotropin Releasing Factor Pathway for Ethanol Regulation of the Ventral Tegmental Area in the Bed Nucleus of the Stria Terminalis. J Neurosci 33: 950–960. [PubMed: 23325234]

Silberman Y, Matthews RT, Winder DG (2013b). A Corticotropin Releasing Factor Pathway for Ethanol Regulation of the Ventral Tegmental Area in the Bed Nucleus of the Stria Terminalis. J Neurosci 33: 950 LP – 960. [PubMed: 23325234]

Sinha R (2008). Chronic Stress, Drug Use, and Vulnerability to Addiction. Ann N Y Acad Sci 1141: 105–130. [PubMed: 18991954]

Sinha R, Fox HC, Hong KA, Bergquist K, Bhagwagar Z, Siedlarz KM (2008). Enhanced Negative Emotion and Alcohol Craving, and Altered Physiological Responses Following Stress and Cue Exposure in Alcohol Dependent Individuals. Neuropsychopharmacology 34: 1198. [PubMed: 18563062]

Van Skike CE, Diaz-Granados JL, Matthews DB (2015). Chronic Intermittent Ethanol Exposure Produces Persistent Anxiety in Adolescent and Adult Rats. Alcohol Clin Exp Res 39: 262–271. [PubMed: 25684048]

Sun N, Cassell MD (1993). Intrinsic GABAergic neurons in the rat central extended amygdala. J Comp Neurol 330: 381–404. [PubMed: 8385679]

Wills TA, Klug JR, Silberman Y, Baucum AJ, Weitlauf C, Colbran RJ, et al. (2012). GluN2B subunit deletion reveals key role in acute and chronic ethanol sensitivity of glutamate synapses in bed nucleus of the stria terminalis. Proc Natl Acad Sci 109: E278 LP–E287. [PubMed: 22219357]

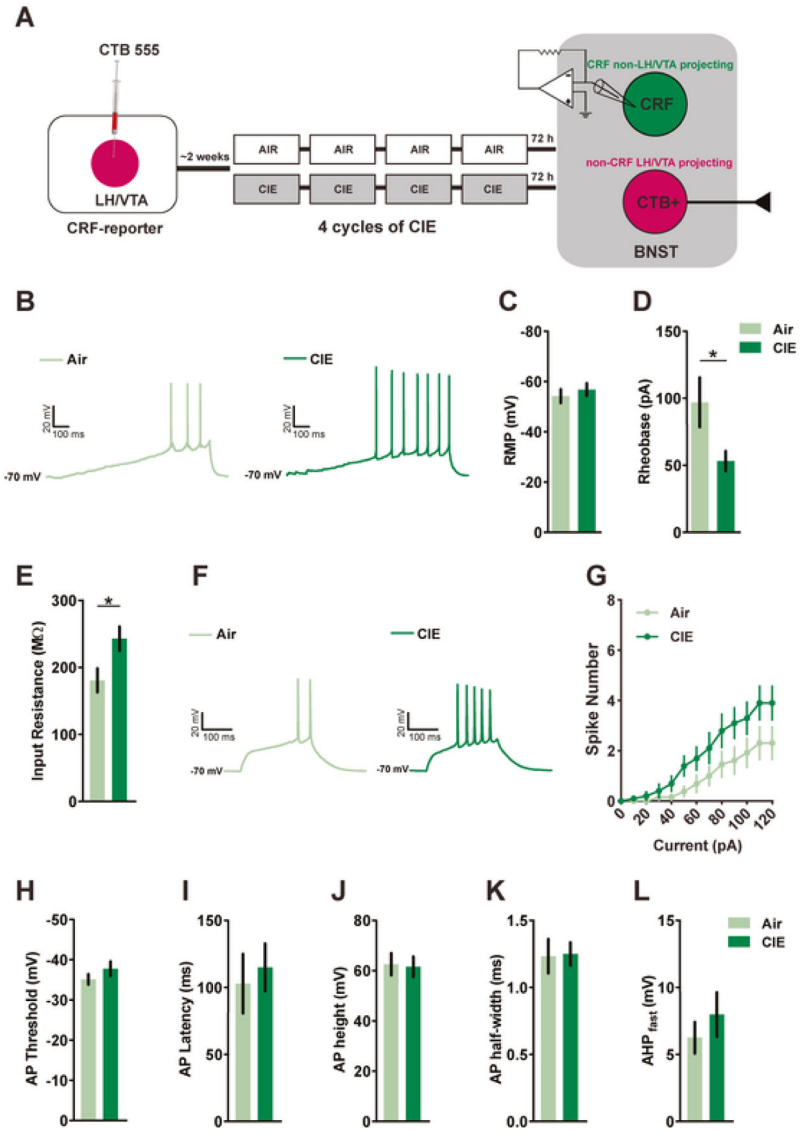

Figure 1. Withdrawal from CIE increases excitability of CRF$^{non\text{-}VTA/LH}$ neurons

A) Experimental timeline for whole-cell recordings from CRF$^{non\text{-}VTA/LH}$ neurons (total of 6 mice in each group) following exposure to 4 cycles of CIE. **B)** Representative data obtained from CRF$^{non\text{-}VTA/LH}$ neurons in Air and CIE mice in response to a 120 pA/s current ramp while injecting a constant current to hold the cells at −70 mV. The minimum current required to fire an action potential (rheobase) was reduced in CIE mice (n=10 cells) when compared to the Air group (**D;** n=13 cells) without any changes **(C)** in the resting membrane potential (RMP; n= 12 cells and n= 8 cells from Air and CIE groups, respectively). **E)** There was a significant decrease in the membrane resistance of CRF$^{non\text{-}VTA/LH}$ neurons following CIE (n= 13 cells in Air and n= 10 cells in CIE). **F)** Representative traces of a CRF$^{non\text{-}VTA/LH}$ neuron in Air and CIE group, respectively, firing action potentials in response to a step protocol of increased current steps of 10 pA/250 ms. **G)** There was a significant interaction between the number of spikes in response to a graded current injection and chronic exposure to ethanol (n= 13 cells in Air and n= 10 cells in CIE). **H)** There was no change in action

potential threshold between the two groups. Chronic ethanol did not alter action potential kinetics as measured by latency, average action potential height, action potential half-width (**I-K;** n= 9 cells in Air; n= 10 in CIE from 6 mice in each group), and fast after hyperpolarization potential (**L;** Air= 8 cells and CIE=9 cells 6 mice in each group). Data expressed as Mean ± SEM.*$p<0.05$.

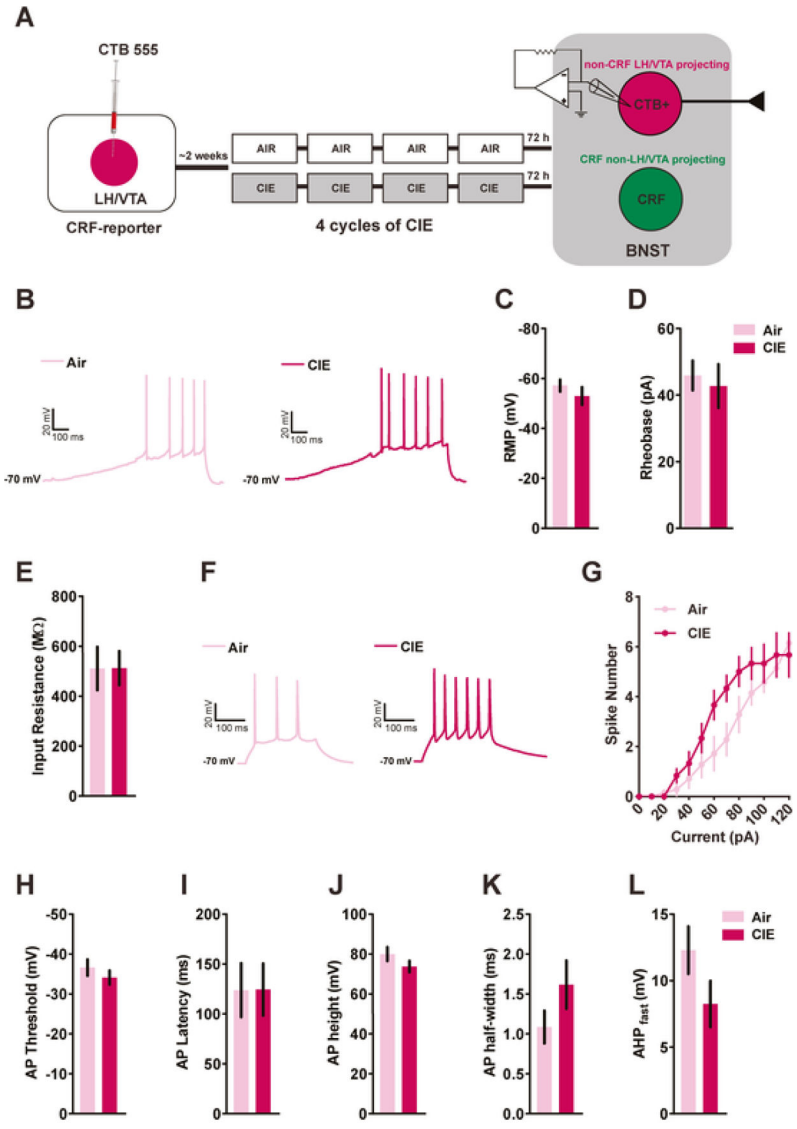

Figure 2. Neuronal excitability of BNST$^{non\text{-}CRF\text{-}proj}$ neurons following withdrawal from CIE

A) Schematics showing timeline for whole-cell recordings from BNST$^{non\text{-}CRF\text{-}proj}$ neurons (4 mice per group) following exposure to 4 cycles of CIE. **B)** Representative traces of BNST$^{non\text{-}CRF\text{-}proj}$ neurons obtained from Air and CIE mice, respectively, in response to a 120 pA/s current ramp while injecting a constant current to hold the cells at −70 mV. **(C)** There was no change in the RMP (n= 7 cells from Air mice; n= 5 cells from CIE mice), rheobase or input resistance **(D-E;** n= 7 cells from Air mice; n= 6 cells from CIE-exposed mice) of BNST$^{non\text{-}CRF\text{-}proj}$ neurons following CIE. **F)** Representative traces of action potentials fired across a range of current steps obtained from the Air and the CIE group. **G)** There was a significant interaction between the number of spikes fired and chronic exposure to ethanol (n= 7 cells Air group; n= 6 cells CIE group). **H)** No change in action potential threshold was observed between the two groups. Similar to CRF$^{non\text{-}VTA/LH}$ neurons, chronic ethanol exposure did not alter action potential kinetics of the BNST$^{non\text{-}CRF\text{-}proj}$ neurons (**I-L)**. Data expressed as Mean ± SEM.*p<0.05.

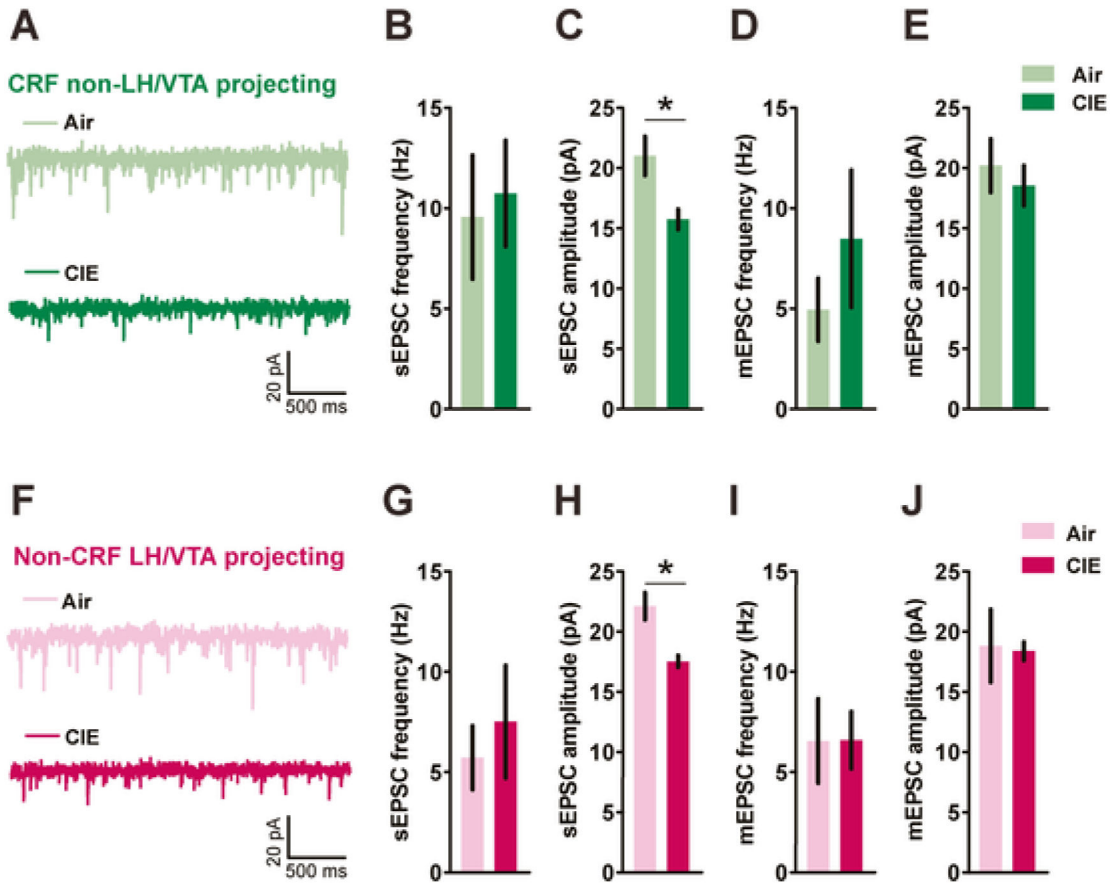

Figure 3. Effects of post-CIE withdrawal on glutamatergic synaptic transmission in both CRF$^{non\text{-}VTA/LH}$ and BNST$^{non\text{-}CRF\text{-}proj}$ neurons

Representative traces of spontaneous excitatory postsynaptic currents (sEPSCs) from CRF$^{non\text{-}VTA/LH}$ neurons (**A**) and BNST$^{non\text{-}CRF\text{-}proj}$ neurons (**F)** post 72h withdrawal from CIE. A reduction in sEPSC amplitude (**C**) but not frequency (**B**) was observed in CRF$^{non\text{-}VTA/LH}$ neurons following CIE (n=12-13 cells from 5 mice in each group). **D-E)** There were no differences in miniature excitatory postsynaptic currents (mEPSCs) in CRF$^{non\text{-}VTA/LH}$ neurons following either air (n= 10 cells from 5 mice) or ethanol (n= 9 cells from 4 mice) exposure. **G)** No difference in sEPSC frequency but a significant reduction in the sEPSC amplitude (**H**) onto BNST$^{non\text{-}CRF\text{-}proj}$ neurons was observed post CIE (n=11-12 cells from 5-6 mice in each group). **I-J)** No effect of CIE on mEPSC transmission onto BNST$^{non\text{-}CRF\text{-}proj}$ neurons (n= 9 cells in Air group versus n= 11 cells in CIE group from 4 mice each). Data expressed as Mean ± SEM.*p<0.05.

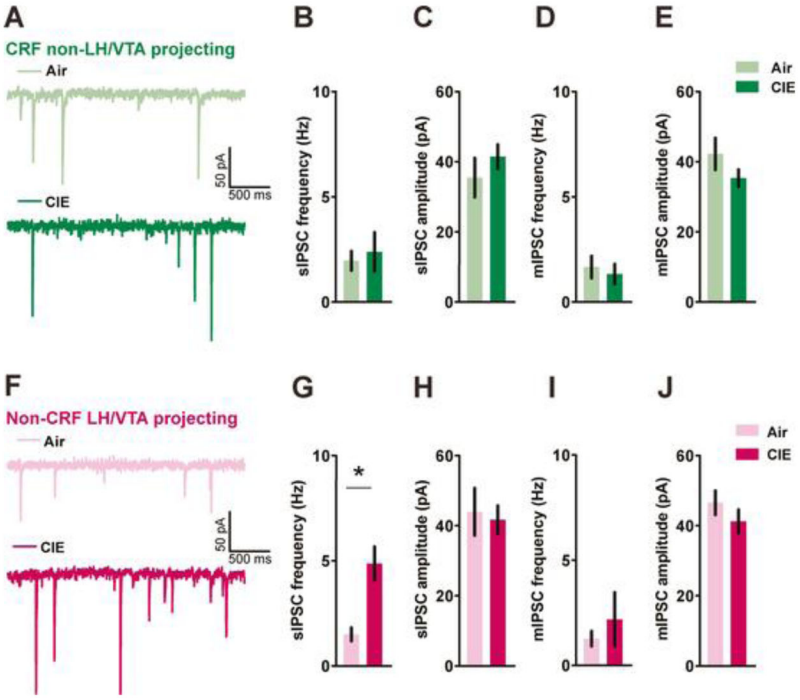

Figure 4. Withdrawal from CIE selectively increases spontaneous inhibitory synaptic transmission in BNST$^{non\text{-}CRF\text{-}proj}$ neurons

Representative traces of spontaneous inhibitory postsynaptic currents (sIPSCs) from CRF$^{non\text{-}VTA/LH}$ (**A)** and BNST$^{non\text{-}CRF\text{-}proj}$ neurons (**F**). There were no between-group differences in sIPSC parameters in CRF$^{non\text{-}VTA/LH}$ neurons (**B-C**; n= 10-11 cells from 5 mice in each group) but a significant increase in sIPSC frequency in the BNST$^{non\text{-}CRF\text{-}proj}$ neurons post CIE (**G-H**; n= 11 cells from 3 air mice and n= 19 cells from 4 CIE mice). No changes were observed in mIPSC parameters in either CRF$^{non\text{-}VTA/LH}$ neurons (**D-E;** n= 9 cells each from 4 air-exposed mice and 5 CIE-exposed mice, respectively) or BNST$^{non\text{-}CRF\text{-}proj}$ neurons (**I-J;** n= 12 cells from 6 Air mice and n= 7 cells from 3 CIE mice) following 4 weeks of CIE. Data expressed as Mean ± SEM.*$p<0.05$.